Transient dopamine neuron activity precedes and encodes the vigor of contralateral movements

Marcelo D Mendonça[1,2], Joaquim Alves da Silva[1,2], Ledia F. Hernandez[3,4,5], Ivan Castela[3,4], José Obeso[3,4,5], Rui M Costa[1,2,6*]

1 - Champalimaud Research, Champalimaud Centre for the Unknown, Lisbon 1400-038

2 - NOVA Medical School | Faculdade de Ciências Médicas, Universidade Nova de Lisboa, Lisbon 1169-056, Portugal.

3 - HM CINAC (Centro Integral de Neurociencias Abarca Campal). Hospital Universitario HM Puerta del Sur, HM Hospitales. Madrid, Spain.

4 - Center for Networked Biomedical Research on Neurodegenerative Diseases (CIBERNED), Carlos III Institute of Health, Madrid, Spain.

5 - Universidad CEU-San Pablo, Madrid, Spain.

6 - Departments of Neuroscience and Neurology, Zuckerman Mind Brain Behavior Institute, Columbia University, New York, NY 10027, USA.

*Correspondence can be addressed to RMC rc3031@columbia.edu

Highlights

- Developed a freely-moving task where mice learn rapid individual forelimb sequences.
- Movement-related DANs encode contralateral but not ipsilateral action vigor.
- The activity of reward-related DANs is not lateralized.
- Unilateral dopamine depletion impaired contralateral, but not ipsilateral, movement vigor.
- **eTOC summary:** Mendonça et al. show that transient activity in movement-related dopamine neurons in substantia nigra pars compacta encodes contralateral, but not ipsilateral action vigor. Consistently, unilateral dopamine depletion impaired contralateral, but not ipsilateral, movement vigor.

Summary

Dopamine neurons (DANs) in the substantia nigra pars compacta (SNc) have been related to movement vigor, and loss of these neurons leads to bradykinesia in Parkinson's disease. However, it remains unclear whether DANs encode a general motivation signal or modulate movement kinematics. We imaged activity of SNc DANs in mice trained in a novel operant task which relies on individual forelimb movement sequences. We uncovered that a similar proportion of SNc DANs increased their activity before ipsi- *vs.* contralateral forelimb movements. However, the magnitude of this activity was higher for contralateral actions, and was related to contralateral but not ipsilateral action vigor. In contrast, the activity of reward-related DANs, largely distinct from those modulated by movement, was not lateralized. Finally, unilateral dopamine depletion impaired contralateral, but not ipsilateral, movement vigor. These results indicate that movement-initiation DANs encode more than a general motivation signal, and invigorate kinematic aspects of contralateral movements.

Keywords: Dopamine, Movement, Substantia Nigra, Laterality, Vigor, Parkinson's Disease, Reward.

Introduction

Choosing which actions to perform in specific contexts is critical for survival. It is also critical to perform these actions at the right time and with the right potency, i.e. force, speed, duration. Basal ganglia circuits, and dopaminergic signaling in these circuits, are critical for the modulation of both movement initiation and movement vigor (Howe et al., 2016; da Silva et al., 2018). Accordingly, one essential feature of Parkinson's Disease (PD), which is characterized by a progressive loss of dopaminergic neurons (DANs) in the Substantia Nigra *pars compacta* (SNc) (Ehringer and Hornykiewicz, 1960), is reduced amplitude (hypokinesia) and slowness of movements (bradykinesia)

Early studies identified that substantia nigra *pars compacta* (SNc) dopaminergic activity was modulated during large reaching movements (Schultz et al. 1983; Romo and Schultz, 1990). More recently, the activity of DANs was found to be transiently modulated around movement onset (Jin and Costa, 2010; Parker et al. 2016; Howe et al. 2016; Collins et al. 2016; Dodson et al. 2016; da Silva et al. 2018), and manipulations of this activity before movement onset had an impact on the probability of movement execution and the vigor of movements (Howe et al. 2016; da Silva et al. 2018). This is supported by well-established observations that chronic DA depletion leads to decreased amplitude, peak force, and speed of movement in PD (Hallett and Khosbin, 1980; Bologna et al., 2016; Mazonni et al., 2007), and also in rodents (Dowd and Dunnett, 2005; Palmiter, 2008; Panigrahi et al., 2015). While many studies of vigor and PD have focused on movement force and speed, the length/duration of movement sequences is also critically affected, and has been less studied. For example, gait bouts of PD patients are characterized not only by a lower speed but also by a reduced number of steps per bout (Shah et al., 2020).

It has been proposed that DA neurons influence movement vigor by modulating the motivation to behave (Niv et al., 2007; Berke. 2018). Behavioral studies in PD revealed that the deficit in movement vigor reflects a reduced probability of committing to more vigorous actions, even when

necessary for obtaining a reward (Mazonni et al., 2007). PD motor signs typically start focally on one side of the body (Monje et al., 2021), contralateral to the most denervated SNc, where movement vigor deficits are observed (Roggendorf et al., 2012). Similarly, unilateral dopamine depletion in mice leads to deficits in contraversive, but not ipsiversive movements (Carli et al., 1985). Striatum is involved in contralateral movements (Schwarcz et al., 1979; Kitama et al., 1991, Tecuapetla et al., 2016), and DANs activity is higher when animals perform contralateral versus ipsilateral choices (Parker et al., 2016). Thus, dopaminergic activity is properly placed to affect movement kinematics in a lateralized way by directly influencing medium spiny neurons (MSNs) excitability (Lahiri et al., 2020).

In this study, we investigate the hypothesis that movement-related DANs signal not only a general motivation to move, but invigorate specific kinematic aspects of contralateral movements. Towards this end, we developed a novel behavioral task where freely moving mice have to perform fast movement sequences using an individual forelimb in order to obtain reward. This paradigm allowed us to investigate movement sequences performed with either forelimb. We imaged the activity of genetically identified SNc DA neurons using one-photon imaging during lever press task performance. We identified distinct populations of SNc DANs with transient activity related to movement *versus* reward. Although a similar proportion of movement-related neurons were observed bilaterally, their activity was higher for contralaterally performed sequences than for ipsilateral ones. Furthermore, this movement-related activity was related to sequence length but only for contralateral sequences. In contrast, reward-related activity was not lateralized. Consistently, unilateral lesion of SNc dopaminergic neurons led to contralateral, but not ipsilateral, forelimb vigor impairment. These results suggest a role of transient dopaminergic activity before movement in invigorating the duration of contralateral movements.

Results

Mice learn to perform rapid single-forelimb lever press sequences

We trained mice (n=8) to perform a fast lever-pressing task where it was required to press a lever at increasingly higher speed in order to obtain a 10% sucrose reward. During the training, spatial constraints in the lever were imposed in order to restrict the accessibility of the lever to only one forelimb (Fig 1A, Supplementary Movie 1, Supplementary Movie 2).

After introducing the animals to the apparatus and 4 days of continuous reinforcement (CRF, one press = one reward), animals were trained at a progressively faster fixed-ratio schedule (FR4, 4 presses = one reward), up to a maximum of 4 presses in less than 1 second. During the FR4 training, the lever was progressively receded to guarantee that it was only accessible to one forelimb (Fig 1A,H, details in the Methods section). Animals were moved across a training schedule of 19 sessions starting with FR4 in 100 seconds and ending with 5 sessions of FR4 in 1 second. Stability of this asymptotic performance, was tested in 30 consecutive FR4/1sec sessions.

With training, the increase in the total number of lever presses (Fig 1B, $F(3,563, 24,94) = 4,514$ $p=0.0086$), paired the increase in the number of presses/minute (reaching 16.76 +- 12.05 presses/minute in the last session, $F(2,443, 17,10) = 4,001$, $p=0.0311$ Supplementary Fig 1A). During this period, animals rapidly started to organize their behavior in self-paced bouts or sequences of lever presses (Fig 1C-G) with the percentage of lever presses performed within a sequence increasing significantly across training ($F(19,102) = 8.643$, $p<0.001$; Fig 1C) until there were almost no single presses occurring in isolation. In the last training session 94.13% +- 4.50 of lever presses occurred within a sequence with 78.85% +- 16.13 of the sequence being composed by more than one LP (Fig 1C inset).

The number of lever presses within a sequence progressively increased ($F(19,109) = 3.269$, $p<0.001$, Fig 1E,G), with the distribution of lever presses per sequence exhibiting a clear peak at 4 lever presses matching the imposed rule (3.69 +- 0.98, $t7=0.8947$, $p=0.400$). Also, as time criteria become more demanding, mice decrease their inter-press intervals (IPIs) up to 0.347 +- 0.276 s (not significantly different from a target of 0.333, $t7=0.1401$, $p=0.8926$ an IPI corresponding to the performance of 4 presses in less than 1 second, $F(19,109) = 2.148$, $p=0.008$, Fig 1I). Consistent with the reduction in the IPI, mice also increased their mean lever press velocity with training (Fig 1K). There was also a progressive reduction of the variability of the IPIs (Fano Factor, Fig 1J, $F(49,308) = 1.118$, $p=0.2840$, post-hoc test for linear trend: $F(1,308)=18.73$, $p<0.0001$).

After the 19 sessions of training, animals were assessed in 30 additional sessions with the criteria of 4 LPs in less than one second, after behavior had asymptote, with no substantial differences noted across these sessions in behavior metrics (Fig 1, Supplementary Fig 1, Supplementary Table 1).

These data indicate that animals learned to shape their behavior to get closer to the target criteria and, after learning, this performance is stable across time. Additionally, animals can be trained to use individual forelimbs (Supplementary Fig 2), allowing us to test ipsi and contralaterally performed movement sequences.

Transient activity of SNc dopaminergic neurons precedes movement sequence initiation

In order to investigate the activity of SNc DANs during the execution of contralateral vs ipsilateral movements we chronically-implanted gradient index (GRIN) lenses above the SNc, and injected a genetically encoded calcium indicator (GCaMP6f) into genetically-identified dopaminergic SNc cells (DAT-Cre), and imaged the activity using a one-photon miniaturized epifluorescence microscope (Ghosh et al., 2011), (Fig 2a-b). Half of the animals (total n=6 mice)

had a virus injection and lens implanted in the left hemisphere and the other half in the right one. We trained these animals in the same task as described above, but with 2 independent sessions each day, where they had to use a separate forelimb (Fig 2D). Each day mice were placed in a box with a lever available on one of the sides (left or right). The session ended after the animal obtained 30 rewards or 30 minutes have passed. After the first session, the animals were removed from this box, and placed in their homecage for a period of 30 to 150 minutes before being trained in a second session in the box, but with the other lever available. The order of limb trained (left or right) was pseudo-randomized across days. Mice were able to perform movement sequences with both forelimbs and, after training, no significant differences in behavioral metrics were noted between the two forelimbs (data summarized in Supplementary Fig 3, Supplementary Table 2, and presented as ipsilateral and contralateral forelimb to the implanted lens). Neural activity was assessed during the phase of asymptotic performance.

Constrained non-negative matrix factorization for endoscope data (CNMF-E) (Zhou et al., 2018) was used to extract activity traces for individual neurons from the microscope video (6 mice, 101 neurons; Fig 2B-C). Neuronal spatial footprints and temporal activity were extracted from conjoined left and right sessions. Then, for all subsequent analysis, a normalized version (z-score) of the scaled, non-denoised version of dF extracted by CNMF-E, was performed for each of the two full sessions (left and right) independently. We created peri-event time histograms using the normalized fluorescence for first press in any lever press sequence and reward consumption for each experimental condition (ipsilateral or contralateral forelimb performance).

In line with previous results (da Silva et al., 2018), we found a population of SNc dopaminergic neurons significantly modulated before movement sequence initiation (~37%) with a small overlap with the population of SNc neurons modulated around reward (~37%) (Fig 2E,F, Supplementary Fig. 4). Some DANs also started their modulation during sequence execution, but this number was lower than those modulated before sequence performance (Only 2-12% of neurons modulated during performance, $F(1,10)=28.82$, $p<0.001$; Supplementary Fig 5A).

Movement-initiation neurons displayed transient increase in activity before both contralateral and ipsilateral forelimb movement sequences (Fig 2G,H Supplementary Fig 5B). However, although a similar proportion of movement-initiation neurons was active before contra and ipsilateral movements (p=0.8021, paired t-test, Fig 2I), the magnitude of the activity of these neurons was significantly higher in the contralateral vs. ipsilateral SNc (p<0.001, unpaired t-test, Fig 2J). This difference in neural activity could not be explained by a difference in the performance of the task as no performance differences were identified between ipsi and contralateral forelimb (Supplementary Fig. 3, Supplementary Table 2).

These data show that although movement-initiation neurons were found bilaterally, activity preceding contralateral limb movements is higher that the activity preceding ipsilateral movements.

DANs encode the vigor of upcoming contralateral, but not ipsilateral, forelimb movements.

We next investigated the relation between the magnitude of the dopamine transients before movement initiation and the vigor of the sequences. We started by dividing the performed sequences into short and long movement bouts (based on the mean sequence duration). The magnitude of the activity of movement-modulated DANs was significantly higher before longer movement sequences than before shorter ones when movements were performed with the contralateral limb (Fig 3A left, n=37 neurons, paired t-test t=4.493, df=36, p<0.0001) but not when performed with the ipsilateral one (Fig 3A right, n=33 neurons, paired t-test t=0.7195, df=32, p=0.4771). This supported the hypothesis that transient SNc activity encode contralateral vigor.

Even accounting for some day-to-day variability in the field of view, *in vivo* calcium imaging permits us to track the same region of interest (ROI) across multiple sessions. This approach allows us to explore if SNc neurons' activity is functionally stable across different performance sessions of highly-trained movements (supporting the argument of a functional identity of specific dopaminergic neurons during task performance in a context of diversity of functions – Fig 2F). To

match neurons across sessions, we used a nearest neighbor approach. For all sessions, a centroid for each ROI was calculated. For each reference centroid, distance from all centroids on the image to be compared was calculated, and the 3 ROIs with the smallest distance were visually inspected for their shape to confirm the matching. Pairing was iteratively performed across the 3 included sessions. We extracted 114 ROIs that were matched in at least 2 sessions (40 ROIs – 35.09% - were matched across the 3 sessions, Fig 3B)

Event-aligned activity of matched neurons was correlated across daily sessions and the results were averaged if matched more than 2 sessions (matched group). The activity of the same neuron was correlated with non-matched neurons from the same animal and averaged across daily sessions (shuffled group). This approach revealed that there is a high correlation of event-aligned activity of spatially mapped neurons (66.7% of neurons had a strong correlation – above 0.5, Fig 3B, Fig 3C) and this similarity was significantly higher than correlations with non-spatially mapped ones (0.677 +- 0.049 vs. 0.149 +- 0.014, paired t-test performed in the Fisher's Z transformed correlation coefficient $t=14.66$, $df=113$, $p<0.0001$, Fig 3D). This analysis suggests that, in general, SNc dopaminergic neurons functional identity remains stable across days while animals perform the learned task.

Matching across days (as performed in Fig 3B) allowed us to study the activity of similar neurons across sessions (Fig 3E) and classify them as vigor-modulated or not. Vigor modulated neurons represented around 22% of contralateral action initiation neurons (Fig 3F). When trials from 3 sessions were considered, activity of movement-initiation neurons was related with contralateral vigor (Fig 3G left, n=37 neurons, paired t-test, $t=2.310$, $df=36$, $p=0.027$), a result that was not present ipsilaterally (Fig 3G right, n=33 neurons, paired t-test, $t=1.120$, $df=32$, $p=0.239$).

These data show that activity in movement-initiation SNc neurons code the vigor of contralateral (in comparison to ipsilateral) performed movement sequences, and their neural identity keeps stable over time.

238 **Reward-related dopamine activity is not lateralized**

239 Modulation around reward was identifiable when mice performed the task either in the ipsi
240 and contralateral conditions (Fig 4A,B). The number of neurons was not significantly different
241 between conditions (Fig 4C, 36.9% +- 5.9 vs. 41.1 +- 14.1, paired t-test: p=0.8003, Fig 4D). The
242 number of reward-modulated neurons (active only after reward consumption) was similar when
243 the action leading to that reward was performed ipsi or contralaterally (~23%, Fig 4F middle,
244 paired t-test: p=0.9235) and no difference was observed in the maximum fluorescence of neurons
245 according to the side of performed action (0.94 +- 0.09 vs. 1.02 +- 0.07 Fig 4F right, t-test:
246 p=0.4760). The overlap between reward-modulated neurons and movement initiation neurons
247 was residual (~2.5% of the total) and significantly lower than the one we would expect by random
248 allocation (Supplementary Fig 6), revealing that movement initiation and reward neurons mostly
249 represent two distinct populations.

250 A second group of neurons was already active before reward consumption and ramped up as
251 animals approached the magazine (Fig 4D, bottom, hereafter called magazine-approach
252 neurons) (Howe et al., 2013). Based on the box design, approach to the magazine could be
253 performed with either an ipsi or a contraversive movement (Fig 4E). While the number of
254 magazine-approach neurons was not significantly different during ipsi or contraversive
255 movements (~15%, paired t-test: p=0.8308) their activity was significantly higher during
256 contraversive movements (1.51 +- 0.19 vs. 0.66 +- 0.19 Fig 4G right, t-test: p=0.0035).

257 These data support that movement initiation and reward modulated neurons in the SNc are
258 not likely the same DAN population and neurons responsive to reward consumption do not have
259 a lateralized representation.

260

261 **Dopaminergic depletion reduces the vigor of contralaterally performed forelimb movement**
262 **sequences**

The results shown above suggest that SNc dopaminergic activity is asymmetric during single forelimb movements, and that its' magnitude is related to the vigor of contra but not ipsilateral sequences. We therefore tested if unilateral loss of dopaminergic neurons in SNc would preferentially affect the vigor of contralateral sequences. To achieve that, we used unilateral striatal injection of 6-hydroxydopamine (6-OHDA), a neurotoxin that selectively affects dopaminergic neurons. It causes rapid degeneration of striatal terminals (within hours after treatment) and changes in SNc DANs markers and cell body structure and numbers are detectable already 3 days after lesion (Stott et al., 2014).

A new group of 14 mice was trained in the task as described in Fig 2D until they reached an asymptotic stage (FR4/1 second). After this, using a stereotaxic approach, injection of 2 uL of 6-OHDA (n=8) or saline (n=6) was performed in dorsolateral striatum in a randomly chosen side (left or right). Post-operative care was performed during the following 7 days and mice did not have access to the operant boxes. After this time period, mice were again placed in the operant boxes and had to perform the task to obtain reward using the same criteria as before treatment (FR4/1 second) (Fig 5A, B).

Unilateral dopamine depletion led to a reduction in the number of presses per sequence (2 Way repeated-measures ANOVA, Time $F(1,7)=68.90$, $p<0.001$, Forelimb $F(1,7)=4.704$, $p=0.0667$, Time x Forelimb $F(1,7)=11.11$, $p=0.0125$, Fig 5C left) and corresponding reduction in the percentage of long/high vigor sequences (2 Way repeated-measures ANOVA, Time $F(1,7)=30.12$, $p<0.001$, Forelimb $F(1,7)=2.087$, $p=0.1918$, Time x Forelimb $F(1,7)=32,45$, $p<0.001$ Fig 5E left). Whereas the contralateral limb to the lesion started to perform smaller sequences (4.12 +- 0.20 to 2.17 +-0,14, Fig 5C left, Multiple comparison after 2-way repeated-measures ANOVA, $p<0.001$) and show a reduced number of long/high vigor sequences (48.82% +- 7.72 to 8.13% +- 3.48, Fig 5E left, Multiple comparison after 2-way repeated-measures ANOVA, $p<0.001$) this was not observed for the limb ipsilateral to the lesion (4.13 +- 0.34 to 3.52 +- 0.39, Fig 5C left, Multiple comparison after 2-way repeated-measures ANOVA, $p=0.138$ and 41.34% +- 5.16 to

37.67% +- 5.67, Fig 5E left, Multiple comparison after 2-way repeated-measures ANOVA, p=0.9725). Regardless of the unilateral dopamine depletion mice kept performing the task with the intended limb (Sup Fig. 7).

The relative mean sequence length (after treatment/before treatment) was significantly different between sides (Fig 5C right, paired t-test, t=3,759, df=7 p=0.007) and significantly different from the unit value (representing no change) only contralaterally (Fig 5C right, one sample t-test, t=11.07, df=7, p<0.001). This result was confirmed by the significant difference in the relative proportion of long sequences between sides (Fig 5E right, paired t-test, t=4,126, df=7 p=0.004, significance from the unit value only identified contralaterally, Fig 5E right, one sample t-test, t=15.46, df=7, p<0.001)

By contrast, injection of saline only led to a small, and non-side specific reduction in the average number of presses/sequence (Fig 5D left, 2 Way repeated-measures ANOVA, Time F(1,5)=7.704, p=0.039, Side F(1,5)=2.007, p=0.216, Time x Side F(1,5)=0.010, p=0.923) without a significant change in the proportion of long sequences (Fig 5F left, 2 Way repeated-measures ANOVA, Time F(1,5)=4.911, p=0.078, Side F(1,5)=0.8281, p=0.405, Time x Side F(1,5)=0.003, p=0.957). When the relative mean sequence length was compared between sides no difference was found (Fig 5D right, paired t-test, t=0.44, df=5, p=0.6755), similar to the lack of a difference in sequence length change (Fig 5F right, paired t-test, t=0.5099, df=5 p=0.6319),

Overall, these data show that unilateral dopamine depletion leads to a reduction in the length of contralaterally performed movement sequences, without impacting the vigor or performance of ipsilateral movements.

Discussion

We found that activity in a subset of SNc dopaminergic neurons encodes the vigor of contralateral actions before movement initiation. Using a novel lateralized task, we unraveled that

315 transient SNc dopaminergic activity precedes the execution of forelimb movement sequences
316 irrespective of the limb performing the sequence. However, this signal was only related to the
317 movement vigor of contralateral (but not ipsilateral) sequences. Also, striatal dopamine depletion
318 disrupted the vigor of contralateral, but not ipsilateral, movement sequences. By contrast,
319 responses of reward-related SNc neurons were bilateral and modulated irrespectively of the side
320 of the preceding action.

321 Laterality is a major topic in nervous system organization, and most attention on nigro-striatal
322 pathway has been placed on the dopaminergic striatal terminals. Although in freely moving
323 animals, striatal dopamine transients are synchronized across hemispheres (Fox et al., 2016),
324 contralateral action response was identified in DA terminals in dorsal striatum (Parker, et al.,
325 2016). SNc neurons have both ipsilateral and contralateral functionally relevant projections
326 (Jaeger et al., 1983), but those ipsilateral to SNc cell bodies are anatomically overrepresented
327 (Poulin et al., 2018). Our data suggest that activity in DANs cell bodies is lateralized, and hence
328 the higher activity in striatal DA terminals observed before contralateral movements are not solely
329 explained by more arborization of SNc neurons to ipsilateral striatum, or enhanced terminal
330 modulation of DA release. Furthermore, and given that dopamine depletion starts asymmetrically
331 by the caudal putamen in PD (Morrish et al., 1996; Monje et al., 2021), these findings have
332 implications for understanding the asymmetry in movement vigor observed in PD (Djaldeti et al.,
333 2006; Mazonni et al., 2007).

334 It has been previously shown that dopamine and its' metabolite 3,4-dihydroxyphenylacetic
335 acid (DOPAC) increase bilaterally in the striatum in relation to speed when rodents ran straight,
336 but contralaterally when they performed circling movements (Freed et al., 1985). This is in line
337 with the asymmetry in SNc neuronal activation we observed, and suggests that asymmetric tonic
338 levels of dopamine in dorsal striatum regulate movement vigor (Schultz, 2002). Furthermore, our
339 results suggest that transient changes in SNc dopamine preceding movement onset, in addition
340 to tonic activity, modulate kinematic aspects of contralateral movements.

Although evidence of laterality is present in movement responses, the same is not true for reward responses. This activity was similar irrespective of the side of the performed action that led to it and started only after reward collection. The lack of laterality of reward responses was also noted in a fiber photometry study in ventral striatum where headfixed mice had to perform an ipsi or contralateral movement in response to a visual stimulus (Moss et al., 2020). This suggests that responses to unpredicted reward represent a more general teaching signal in the brain, and not solely related to the action performed to obtain the reward.

Although efforts have been made to unify observations of movement and reward responses in DANs, under classic RPE model, some studies suggest that movement signals are modulated distinctly from RPE (Lee et al., 2019). The results presented here also suggest that movement signals and reward-related signals can be independently modulated. If movement-related signals would reflect learned action value, we would not expect a difference in magnitude of activity based on which limb was used to perform the actions - as reward prediction is similar for both left and right limb performance of action sequences. Furthermore, we would not expect that magazine-approach activity (Howe et al., 2013) would be higher for contraversive than ipsiversive movements, as again these actions have the same expected value. These observations do not argue that dopamine neurons do not encode an RPE, just that not all dopamine neurons necessarily encode an RPE. Facing the high dimensionality of an organism behavior, error signals could be differently decomposed according to the condition (Diuk et al., 2013) or different state information may be carried by dissociable parallel circuits (Takahashi et al., 2016; Lau et al., 2017). However, they substantiate the existence of a population of SNc DA neurons directly involved in movement and movement invigoration.

The findings here deserve further expansion regarding some aspect of PD etiopathogenesis. First, the involvement of distinct SNc populations in movement initiation vs. reward is in keeping with the notion of selective vulnerability of nigrostriatal degeneration and the origin of motor versus neuropsychiatric manifestations such as depression, anxiety or apathy (Weintraub et al., 2015).

Second, the finding that SNc activity is directly linked with the execution and vigor of a learned movement sequence implicates that, contrary to classic understanding (DeLong et al., 1983), the nigrostriatal dopaminergic system may continue to be activated and engaged during the performance of routine, automatic actions. Such neurons in the ventrolateral SNc are the first and most affected in PD and accordingly, the findings here agree with the hypothesis of high metabolic demand and overuse as critical vulnerability factor underlying the onset of neurodegeneration (Hernandez et al, TINS, 2019). Thus, clarifying if there is a link between genetic heterogeneity and functional phenotypes in these dopaminergic neurons could provide valuable resources to better understand the spectrum of clinical manifestations in PD and, more importantly, to define the origin of selective neuronal dopaminergic degeneration in PD.

386 **Acknowledgements**

387

388 We thank Ana Vaz and Catarina Carvalho for mouse colony management, Thomas Akam and
389 Hélio Rodrigues for help in behavioral box development and implementation, and the
390 Champalimaud Hardware Platform (Filipe Carvalho, Artur Silva and Dário Bento) for support in
391 the development of the behavioral hardware setup. We thank Cristina Alcácer and Nuno Loureiro
392 for their contributions during the 6-OHDA experiments. This work was supported by Fundação
393 para a Ciência e Tecnologia (FCT) through a doctoral fellowship (SFRH/BD/119623/2016 to
394 MDM) and Fundação Luso-Americana para o Desenvolvimento (FLAD) by a visiting student
395 fellowship (2018/31 to MDM); by a doctoral fellowship from the Gulbenkian Foundation (to JAdS),
396 by a Marie Curie Fellowship (MSCA-IF-RI 2016; to LFH), by a predoctoral grant by Spanish
397 Ministry of Innovation and Science (BES-2016-077493 to IC), by ERA-NET, ERC (COG 617142),
398 HHMI (IEC 55007415), National Institute of Health (5U19NS104649), and the Simons-Emory
399 International Consortium on Motor Control to RMC. Further support was obtained from the
400 research infrastructure Congento, co-funded by Lisboa2020 and FCT (LISBOA-01-0145-FEDER-
401 022170).

402

403 Author Contributions

404 MDM, JAdS and RMC designed experiments and conceptualized analysis. MDM, JAdS and LFH
405 performed behavioral experiments. MDM, LFH and IC performed calcium imaging experiments.
406 MDM performed analysis with contribution from JAdS. MDM wrote the original draft with JAdS
407 and RMC which was critically reviewed by the other authors. RMC and JO supervised the work.

408

409

Methods:

Experimental Model and Subject Details

All experiments were approved by the Portuguese Direcção Geral de Veterinária and Champalimaud Centre for the Unknown Ethical Committee and performed in accordance with European Union Directive for Protection of Vertebrates Used for Experimental and other Scientific Ends (86/609/CEE and Law No. 0421/000/000/2014). Male C57BL/6J mice were tested between 2 and 4 months old. For calcium imaging studies, the male DAT-IRES:Cre (Dopamine Transporter-Internal Ribosome Entry Site-linked Cre recombinase gene) mouse line from Jackson Labs Stock 006660 (The Jackson Laboratory; B6.SJL-Slc6a3tm1.1(Cre)Bkmn/J) was used. These mice have Cre recombinase expression directed to dopaminergic neurons, without disrupting endogenous dopamine transporter expression. Genotype was confirmed by polymerase chain reaction (PCR) amplification. Sample sizes are detailed in the Results and/or figure legends.

Virus injections and lens placement.

Mice were kept in deep anaesthesia using a mixture of isoflurane and oxygen (1-3% isoflurane at 1l/min) and the procedure was conducted in aseptic conditions.

The mouse head was stabilized in the stereotaxic apparatus (Koft), a skin incision was performed to expose the skull, connective and muscle tissue was carefully removed and the skull surface was leveled at less than 0.05mm by comparing the height of bregma and lambda, and also in medial-lateral directions. Unilateral virus injection was performed using a glass pipette with GCaMP6f stock viral solution (AAV2/5.SYN.FlexGCaMP6fWPRE.SV40 - University of Pennsylvania). For imaging, 1 ul of virus solution was injected in the right (n=3) of the left (n=3) substantia nigra compacta at the following coordinates: -3.16 mm anteroposterior, 1.40mm lateral from bregma and 4.20 deep from the brain surface. The injection was done using a Nanojet II or

436 Nanojet III (Drummond Scientific) with a rate of injection of 4.6 nl every 5s. After the injection was
437 finished, the pipette was left in place for 10-15 minutes. The virus solution was kept at -80 ºC and
438 thawed at room temperature just before the injection.
439 A 500-um diameter, 8.2-mm long gradient index (GRIN) lens (GLP-0584, Inscopix) was
440 implanted at the same coordinates as the injection. Before the lens was lowered, a blunt 28 G
441 needle was lowered to 3 mm deep from the brain surface to facilitate the lowering of the GRIN
442 lens. The GRIN lens was then lowered (4.2 mm deep). The lens was fixed in place using
443 cyanoacrilate, quick adhesive cement (C&B Metabond) and black dental cement (Ortho-Jet).
444 Three weeks after surgery, the mouse was anaesthetized and fixed with head bars. A baseplante
445 (BPC-2, Inscopix) attached to a mini epifluorescence microscope (nVista HD, Inscopix) was
446 positioned above the GRIN lens. To correctly position the baseplate, brain tissue was imaged
447 through the lens to find the appropriate focal plane using 40% LED power, a frame rate of 10 Hz
448 and a digital gain of 4. Once the focal plane was set, the baseplate was cemented to the rest of
449 the cap using the same dental cement. Imaging started 2–3 days after this final step.
450
451 **Single-limb fast FR4 operant task.**
452 Animals were trained using 14x16 cm custom-built operant chambers placed inside sound
453 attenuating boxes. PyControl, (https://pycontrol.readthedocs.io), a behavioral experiment control
454 system built around the Micropython microcontroller, was used to control and detect events and
455 supply rewards. The custom-built boxes had in their design a retractable lever.
456 At the beginning of each session there was the onset of a light, and the animals were required
457 to perform a sequence of presses at a minimum frequency in order to obtain a sucrose reward.
458 Sucrose solution (10%) was delivered through the opening of a solenoid (LHDA1231515H, Lee
459 Company). Sucrose solution was delivered through a tube into the magazine (5µl per reward).
460 Licks were detected using an infrared beam and through a side camera, mouse position in the
461 box was monitored through a camera placed on the top of the box.

462 Mice were placed on food restriction throughout training, and fed daily after the training
463 sessions with approximately 1.5 - 2.5g of regular food to allow them to maintain a body weight of
464 around 85% of their baseline weight. To facilitate learning, animals were initially exposed to one
465 session of magazine training where sucrose would be available on a random time schedule, and
466 to three to four sessions of continuous reinforcement schedule (CRF) before training, where single
467 lever presses would be reinforced. In the following sessions animals were reinforced if they
468 performed a sequence of 4 consecutive presses (Fixed Ratio 4, FR4) in a particular time window
469 (FR4/Xs, fixed-ration four within X seconds). The duration of time required to perform the four
470 lever presses was reduced across sessions from 100 seconds to 20 s, 8 s, 4 s, 2 s and finally 1s.
471 To shape animals to use only one of the forelimbs the lever was progressively retracted and the
472 slit thought which the forelimb accessed the lever was reduced with a custom-built piece.
473 In the imaging group, animals performed the task 2 times/session - one with the lever in the
474 left side of the box and the other with the lever in the right - that were randomized throughout the
475 training. Task ended after 30 minutes on each side or when the animals obtained 30 rewards.
476 The lever was equipped with a digital 9-axis inertial sensor with a sampling rate of 200 Hz
477 (MPU-9150, Invensense) assembled on a custom-made PCB and connected to a computer via a
478 custom-made USB interface PCB (Champalimaud Foundation Hardware Platform). Lever velocity
479 was extracted from this sensor.
480 Timestamps from the behavioral task were synchronized with calcium imaging data using TTL
481 pulses sent from the behavioral chambers to the Inscopix data acquisition system via a BNC
482 cable.
483
484 **GCaMP6f imaging using a mini-epifluorescence microscope**
485 Mice were briefly anaesthetized using a mixture of isoflurane and oxygen (1% isoflurante at
486 1L/min) and the mini-epifluorescence microscope was attached to the baseplate. This was
487 followed by a period of 15-20 min of recovery in the home cage before starting the experiments.

Fluorescence images were acquired at 10 Hz and the LED power was set 40-60% with a gain of 4. Image acquisition parameters were always set to the same parameters between sessions to be able to compare the activity recorded. Six GCaMP6f-expressing DAT-Cre mice were imaged during the FR4/1s task in 3-5 consecutive days.

Calcium image processing and analysis.

GCaMP6f image processing

All fluorescence movies were initially processed using the Mosaic Software (v. 1.2.0, Inscopix). Two different movies were collected on the same day (one for ipsi and one for contralateral forelimb). As the epifluorescence microscope was not removed during this period, movies were concatenated for the next analysis step. First, all frames were spatially binned by a factor of 4. To correct the movie for translational movements and rotations, frames were registered to a reference image consisting of an average of the raw fluorescence movie.

Extraction of calcium signals

We implemented the 'constrained non-negative matrix factorization for endoscopic data' (CNMF-E) framework for our calcium imaging analysis. This framework is an adaptation of the CNMF algorithm that can reliably deal with the large fluctuating background from multiple sources in the data, and enable accurate source extraction of cellular signals. It include four steps: 1) initialize spatial and temporal components of single neurons without the direct estimation of the background, 2) estimate the background given the estimated spatiotemporal activity of the neurons; 3) update the spatial and temporal components of all neurons while fixing the estimated background fluctuation, 4) iteratively repeat step 2 and 3.

CNMF-E only identifies regions of interest that are active in the condition.

After analysis, data from the videos were separated in ipsi and contralateral videos. Further calcium imaging analyses were performed on standardized scores (z-score) of each session.

Criteria to identify lever-press-related and reward-related DANs using GCaMP6f imaging.

We constructed a PETH for each neuron trace spanning from −8 to 6 s from lever press onset for the first press and for the first lick after reward. Distributions of the PETH from -8 to -3 s before the event were considered baseline activity. We then searched each PETH during a determined epoch for bins that were significantly different from the baseline. A significant change in fluorescence was defined as at least two consecutive bins with fluorescence higher than a threshold of 99% above the baseline. For first-press modulated neurons, a window from -2 to 0 s was used. For rewarded lick modulated neurons a window from 0 to 1 s was used.

For each neuron, maximum activity in specific time-windows was calculated by the maximum of a moving average of 3 bins. The time window was -2 to 0 for lever press, 0 to 1 for neurons modulated after reward and -1 to 0 for neurons modulated before reward.

Cell pairing across sessions

Analysis of matched cells between different days/sessions was based on a nearest neighbors method. For all sessions, a centroid for each ROI was calculated. For each reference centroid, distance from all centroids on the image to be compared was calculated, and the 3 ROIs with the smallest distance were visually inspected for their shape to define a match. Alignments were performed to 4 events: First lever press and Reward in the ipsi and contralateral situations. The calcium-signal from -10 to +6 seconds after the event was used to calculate the correlation coefficients for individual ROIs across days in the 4 conditions. If the neuron was matched in the 3 days, the 3 possible correlation coefficients were calculated and averaged. Then the maximum value was extracted. As a control, we correlated each ROI with all ROIs in the field of view (FOV) of the same animal on the comparison day. The maximum value was extracted and then averaged across units. Correlation values were transformed for each point using Fisher's Z statistic, then the samples were averaged, and back-transformed into a weighted correlation.

PETH correlation across sessions.

For each ROI, 4 PETHs were built as previously described: For the ipsilateral and contralateral conditions 2 events were considered (lever press and rewarded licks). For each ROI pair the correlation between these 4 events was performed. The one with the maximum correlation was identified and this value extracted. This process was repeated when matching occurred across the 3 sessions, and average value between the 3 matchings (A and B, A and C and B and C) was computed. These are the values for matched ROIs in figure 3B.

As a control, we ran the same analysis, but instead of using the matched ROI we used all ROIs from the same animal, in a different session. We then calculated the average of the maximum correlations as previously described.

Sequence length analysis

Movement sequences were divided into short and long sequences by the mean number of presses/sequence of each animal. For each movement sequence, maximum fluorescence in the period -2 to 0 seconds before the first lever press was calculated as previously described.

A neuron was classified as vigor related if it's activity in longer sequences was significantly different ($p<0.05$, unpaired t-test) from the activity in shorter sequences.

Striatal injection of 6-OHDA or Saline and post-operative care

As in virus injections, mice were kept in deep anaesthesia using a mixture of isoflurane and oxygen (1-3% isoflurane at 1l/min) and the procedure was conducted in aseptic conditions.

The mouse head was stabilized in the stereotaxic apparatus (Koft), a skin incision was performed to expose the skull, connective and muscle tissue were carefully removed and the skull surface was leveled at less than 0.05mm by comparing the height of bregma and lambda, and also in medial-lateral directions. 6-Hydroxydopamine hydrochloride (Sigma Aldrich AB, Sweden)

was dissolved at a fixed concentration of 3.2 µg/µl free-base in 0.02% ice-cold ascorbic acid/saline and used within 2 h. Injection of 2 ul of 6-OHDA or saline was performed in the dorsolateral striatum +0.5 mm anteroposterior and ±2.5 mm lateral from bregma and 3.0 mm deep from brain surface. Injection was done through a glass pipette using a Nanojet II with a rate of injection of 4.6 nl every 5s. After the injection was finished, the pipette was left in place for 10-15 minutes.

After surgery, food restriction was reduced (with each animal having access to up 4 mg of food pellets/day). Mice that showed weight loss were hand-fed (i.e. they were presented with the food while being held by the hands of the investigator) and DietGel Boost was placed in their boxed up to 4 days after surgery. In order to avoid competition for the food, weaker mice were placed in cages other than those containing unimpaired mice. The postoperative survival rate was 100%.

Sequence length analysis

Movement sequences were divided into short and long sequences according to mean number of presses/sequence before striatal injection of 6-OHDA or Saline.

Anatomical verification

Animals were euthanized after completion of the behavioural tests. First animals were anaesthetized with isoflurane, followed by intraperitoneal injection of ketamine-xylazine (5 mg/kg xylazine; 100 mg/kg ketamine). Animals were then perfused with 1% phosphate buffered saline (PBS) and 4% paraformaldehyde and brains were extracted for histological processing. Brains were kept in 4% paraformaldehyde overnight and then transferred to 1x PBS solution. Brains were sectioned coronally in 50-um slices (using a Leica vibratome VT1000S) and kept in PBS before mounting or immunostaining.

Images were taken using a wide-field fluorescence microscope (Zeiss AxioImager).

592 **Quantification and statistical analysis**

593 Data is presented as mean ± standard error of mean (SEM) and statistical significance was
594 considered for $p < 0.05$. Statistical analysis was conducted using GraphPad Prism 8 (GraphPad
595 Software Inc., CA) and MATLAB statistical toolbox (The MathWorks Inc, MA). One-way or two-
596 way ANOVAs were used to investigate main effects, and Bonferroni-corrected post-hoc
597 comparisons performed whenever appropriate. Paired or unpaired t-tests were used for planned
598 comparisons. Details for statistical tests are presented in supplementary Table S1. Statistical
599 methods were not used to pre-determine sample size

Key Resources Table

Reagent or Resource	Source	Identifier
Bacterial and Virus strains		
AAV5.SYN.FlexGCaMP6fWPRE.SV40	UPENN	AV-5-PV2822
Chemicals, Peptides, and Recombinant Proteins		
Sucrose	Sigma-Aldrich	Cat# 84099
6-Hydroxydopamine hydrobromide	Sigma-Aldrich	Cat# H116
Experimental Models: Organisms/Strains		
Mouse: Slc6a3$^{tm1(cre)Xz/J}$ (DAT-Cre)	Jackson Laboratories	020080
Mouse: C57BL6	Champalimaud Centre Vivarium	N/A
Software and Algorithms		
CNMF-e	Klaus et al, 2017; Pnevmatikakis et al, 2016	N/A
Bonsai-Open Ephys	Lopes et al, 2015	https://open-ephys.org/bonsai
pyControl	pyControl developers	https://pycontrol.readthedocs.io
Matlab 2016b, Matlab 2018b	MathWorks	https://www.mathworks.com/products/matlab.html

Figure Legends

Figure 1: A novel task for assessment rapid single-forelimb lever press sequences.

A) Schematics of the training schedule. Training starts with a first session of Magazine Training (MT) followed by 4 sessions of continuous reinforcement schedule (CRF) where each press leads to one reward. After a training period of 19 days of FR4 of increasing time constraint (from 4 presses in 100 seconds up to 1 second) and progressive lever retraction to lead to single forelimb lever press (LP). Animals were moved to a performance phase during 30 days, where 4 lever presses performed in less than one second led to a reward. **B)** With training, the total number of Lever Presses increased and **C)** animals rapidly started to organize their behavior in self-paced bouts or sequences of lever presses, until there were almost no single presses occurring. **D)** In the performance stage about 60% of sequences were rewarded as animals reorganize their behaviour **G)** and start to perform lever press sequences of 4-5 presses **E)**.

F) Example of sequences performed by a representative animal, aligned at the time of sequence initiation. Individual lever presses are marked as black ticks, the full sequence duration is shaded in grey and the IPIs that meet the session minimum target are shaded in blue. **H)** Representative frames collected from a high-speed (120 fps) camera during sequence performance. **I)** With training mice decrease the Inter-press interval to a mean of 0.347 seconds. The reorganization of IPIs distribution (*Inset)* happens during training. **J)** Variability of the inter-press interval decreases while press velocity increases across training **K)**.

(Error bar denotes S.E.M.) *p<0.05; **p<0.01; ***p<0.001; **** p<0.0001. For detailed statistical analysis, see Table S1.

Figure 2: SNc dopaminergic neurons are transiently active before movement sequence initiation. A) In 6 DAT-IRES:Cre mice, a miniature epifluorescence microscope was used for deep-brain calcium imaging from SNc dopaminergic neurons during task performance. **B)** Field

of view (projection of pixel standard deviation) of a DAT-Cre mouse expressing GCaMP6f in the SNpc. Regions of interest (ROIs) correspond to traces in C. **C)** Example traces obtained using the CNMF-E algorithm during the FR4 task. ROIs #1 and #5 are examples of units modulated before first lever press - gray lines - and ROIs #2 and #4 are examples of units modulated after reward - red lines. **D)** Schematics of the training schedule used for this set of experiments. Mice were trained in a pseudo-randomized order across different training days alternating between starting with the ipsi- or the contralateral forelimb. **E)** Activity of all recorded ROIs from one session aligned to the first contralateral lever press (left) and to the beginning of reward consumption (right). **F)** Venn diagram representing contralateral first press and reward-related neurons. **G)** PETH of positively modulated neurons for first press and reward (bottom) and corresponding heat maps (top). **H)** Venn diagram representing first press modulated neurons when action was performed by contralateral (blue, same number as in E) and ipsilateral (red) forelimb. **I)** PETH of positively modulated neurons for first press contralateral (blue) and ipsilateral (red) (bottom) and corresponding heat map for ipsilateral neurons (top). **J)** Percentage of positively modulated neurons before first lever press per mouse, comparing contralateral and ipsilateral forelimb (NS, $p = 0.57$, paired t-test). **K)** Maximum fluorescence before first lever press of positively modulated neurons when the action was performed with the contralateral and ipsilateral forelimb (Contralateral, n=37 neurons, Ipsilateral, n=33 neurons, *** $p<0.001$, unpaired t-test). Data are presented as mean ± SEM. *$p<0.05$; **$p<0.01$; ***$p<0.001$; **** $p<0.0001$. For detailed statistical analysis, see Table S1.

Figure 3: Transient SNc activity before the first lever press encodes the vigor of contralateral movement sequences. A) Sequences were classified as short and long sequences based on mean value for each animal. Maximum fluorescence before first lever press of the movement neurons described in figure 2 in long and short sequences performed by contralateral (left panel, n=37, $p<0.001$) and ipsilateral forelimb (right, n=33, $p=0.9297$). **B)**

Matching of ROIs identified across 3 sessions of performance. Only ROIs that were matched in at least 2 of 3 sessions were plotted (left). Heatplot showing the average cross-days correlation of matched neurons PETHs and maximum cross-days correlation of each ROI with all ROIs of the same animal across days as a control (right). **C)** Example PETHs of 3 ROIs in different sessions disclosing the similarities in average neural activity. **D)** Histogram of the cross-days correlations represented in panel C). (n=114 ROIs *** p<0.001, paired t-test). **E)** Example of a contralateral movement-modulated ROI identified across the 3 sessions. PETHs divided by longer sequences (dark blue) and shorter sequences (light blue). Insets with the maximum activity before movement initiation for all long (dark blue) and short (light blue) sequences performed in that session. Right: Maximum activity before movement initiation in all trials of the 3 sessions (p<0.001, unpaired t-test). This strategy was used to identify vigor modulated neurons in panel F). **F)** Vigor modulated neurons: Positively-modulated 13.51% in the contralateral, 6.06% in the ipsilateral (p=0.1960; Fisher exact test); Negatively-modulated: 8.10% in the contralateral, 3.03% in the ipsilateral. **G)** Maximum fluorescence before first lever press of neurons identified in Fig 2 and panel A) accounting for trials in the 3 sessions. Left: Contralateral; Right: Ipsilateral. *p<0.05; **p<0.01; ***p<0.001; **** p<0.0001. For detailed statistical analysis, see Table S1.

Figure 4: Activity of reward-modulated neurons is not lateralized A) Heat maps of neurons with responses around reward when animals performed the task with the ipsilateral and contralateral forelimb. **B)** Venn diagram representing these neurons when reward is collected after performing a contraversive (yellow) and ipsiversive (blue, same number as in 2F) movement. **C)** Percentage of positively modulated neurons in the contra- and ipsiversive conditions (p = 0.80, paired t-test). Data are presented as mean ± SEM. **D)** Example of the 2 types of responses identified around reward: reward-modulated neurons (top) and magazine approach neurons (bottom). Left - Activity heatmap per trial; Right - PETH of that neuron. **E)** Top view of mouse position when pressing the lever and consuming reward in situations where it performs a

685 contraversive (top) and ipsiversive (bottom) movement. **F)** Activity of reward modulated neurons
686 after a contraversive (blue) or ipsiversive (red) movement: PETH of reward modulated neurons
687 (left), percentage of modulated neurons per mouse (n=6, 25.88% +- 15.40 vs. 22.80% +- 8.84,
688 p=0.8902, paired t-test) and Maximum fluorescence after reward consumption (right) (Ipsiversive,
689 n=27 neurons, Contraversive, n=19 neurons, p=0.4860, unpaired t-test). **G)** Activity of magazine-
690 approach neurons after a contraversive (blue) or ipsiversive (red) movement: PETH of magazine-
691 approach neurons (left), percentage of modulated neurons per mouse (n=6, 15.20% +- 5.85 vs.
692 14.14% +- 4.47, p=0.9125, paired t-test) and Maximum fluorescence (right) (Ipsiversive, n=12
693 neurons, Contraversive, n=22 neurons, **p=0.0035, unpaired t-test).
694
695 **Figure 5: Dopamine depletion disrupts contralateral vigor**. **A)** A new group of mice (n=14)
696 was trained in the task performing actions with each forepaw. After a plateau performance was
697 reached, mice were injected with 6-OHDA or saline unilaterally in the striatum and retested after
698 the lesion. **B)** Example of performance with contra- and ipsilateral forelimbs to the lesion side,
699 before (black) and after (purple) treatment of a mouse injected with 6-OHDA (top) and saline
700 (bottom). Intra-striatal treatment with 6-OHDA leads to a redistribution of number of
701 presses/sequence performed on the contralateral forelimb with the performance of sequences.
702 **C)** Change in the number of presses/sequence for 6-OHDA treated animals. Left) Number of
703 presses/sequence across the 4 conditions (Time: Before/After and Forelimb: Contra/Ipsilateral)
704 for 6-OHDA treated animals. There was an effect for Time and an interaction between Forelimb
705 and Time conditions. 2 Way repeated-measures ANOVA, Time $F(1,7)=68.90$, $p<0.001$, Forelimb
706 $F(1,7)=4.704$, $p=0.0667$, Time x Forelimb $F(1,7)=11.11$, $p=0.0125$. Post-hoc tests revealed a
707 significant difference in the before/after condition in the contralateral forelimb (4.12 +- 0.20 to 2.17
708 +-0,14, multiple comparison test after 2-way repeated-measures ANOVA, $t(7)=6.835$, $p<0.001$)
709 but not ipsilaterally (4.13 +- 0.34 to 3.52 +-0.39, multiple comparison test after 2-way repeated-
710 measures ANOVA, $t(7)=2.121$, $p=0.1380$). Right) Ratio of presses/sequence after treatment,

normalized to the one before treatment for both ipsi- and contralateral forelimbs. There was a significant difference between ipsi and contralateral change (paired t-test, t(7)=3.759, p=0.0071) N=8. While contralaterally the change was significantly different from the unit value (one sample t-test vs. 1: t(7)=11.07, p<0.0001), ipsilaterally no significant difference was found (one sample t-test vs. 1: t(7)=2.281, p=0.0565). **D)** Change in the number of presses/sequence for saline treated animals. Left) Number of presses/sequence across the 4 conditions (Time: Before/After and Forelimb: Contra/Ipsilateral) for saline treated animals. There was only small effect for Time. 2 Way repeated-measures ANOVA, Time: F(1,5)=7.704, p=0.0391, Forelimb: F(1,5)=2.007, p=0.2157, Time x Forelimb: F(1,5)=0.01041, p=0.9227. There was not any significant change in the number of presses/sequence after saline treatment either contralaterally (3.40 +- 0.35 to 2.73 +- 0.33, multiple comparison test after 2-way repeated-measures ANOVA, t(5)=1.408, p=0.3885) or ipsilaterally (3.06 +- 0.31 to 2.46 +- 0.45, multiple comparison test after 2-way repeated-measures ANOVA, t(5)=1.264, p=0.4552). Right) Ratio of presses/sequence after treatment, normalized to the one before treatment for both ipsi- and contralateral forelimbs. There wasn't any significant difference between ipsi and contralateral change (paired t-test, t(5)=0.4441, p=0.6755). **E)** Change in the percentage of Long Sequences/All Sequences for 6-OHDA treated animals. Long Sequences are defined as sequences with a number of presses higher than the mean number of presses on baseline condition for each forelimb (i.e. the number calculated in panels C and D). Left) Percentage of Long Sequences/All Sequence across the 4 conditions (Time: Before/After and Forelimb: Contra/Ipsilateral) for 6-OHDA treated animals. There was an effect for Time and an interaction between Forelimb and Time conditions. 2 Way repeated-measures ANOVA, Time F(1,7)=30.12, p<0.001, Forelimb F(1,7)=2.087, p=0.1918, Time x Forelimb F(1,7)=32,45, p<0.001. Post-hoc tests revealed a significant difference in the before/after condition in the contralateral forelimb (48.82% +- 7.72 to 8.13% +- 3.48, t(7)=8.854, p<0.001) but not on ipsilateral forelimbs (41.34% +- 5.16 to 37.67% +- 5.67, t(7)=0.799, p=0.9725). Right) Ratio of long sequences after treatment, normalized to the one before treatment

for ipsi- and contralateral forelimbs. There was a significant difference between ipsi and contralateral change (paired t-test, t(7)=4.126, p=0.0044). While contralaterally the change was significantly different from the unit value (one sample t-test vs. 1: t(7)=15.46, p<0.0001), ipsilaterally no significant difference was found (one sample t-test vs. 1: t(7)=0.210, p=0.8397). **F)** Change in the percentage of Long Sequences/All Sequences for saline treated animals. Left) Percentage of Long Sequences/All Sequence across the 4 conditions (Time: Before/After and Forelimb: Contra/Ipsilateral) for saline treated animals. There were no significant changes with saline treatment (2 Way repeated-measures ANOVA, Time F(1,5)=4.911, p=0.078, Side F(1,5)=0.8281, p=0.405, Time x Side F(1,5)=0.003, p=0.957; Contralateral: 45.87% +- 7.11 to 30.40% +- 14.40; Ipsilateral: 37.35% +- 4.72 to 20.69% +- 8.20). Right) Ratio of long sequences after treatment, normalized to the one before treatment for ipsi- and contralateral forelimbs. There wasn't any significant difference between ipsi and contralateral change (paired t-test, t(5)=0.5099, p=0.6319). Data are presented as mean ± SEM. *p<0.05; **p<0.01; ***p<0.001; *** p<0.0001. For detailed statistical analysis, see Table S1.

References:

Andén NE, Dahlström A, Fuxe K, Larsson K. Functional role of the nigro-neostriatal dopamine neurons. Acta Pharmacol Toxicol (Copenh). 1966;24(2):263-274.

Berke JD. What does dopamine mean?. Nat Neurosci. 2018;21(6):787-793.

Birkmayer W, Hornykiewicz O. [The L-3,4-dioxyphenylalanine (DOPA)-effect in Parkinson-akinesia]. Wien Klin Wochenschr. 1961 Nov 10;73:787-8.

Bologna M, Leodori G, Stirpe P, Paparella G, Colella D, Belvisi D, Fasano A, Fabbrini G, Berardelli A. Bradykinesia in early and advanced Parkinson's disease. J Neurol Sci. 2016 Oct 15;369:286-291.

Carli M, Evenden JL, Robbins TW. Depletion of unilateral striatal dopamine impairs initiation of contralateral actions and not sensory attention. Nature. 1985 Feb 21-27;313(6004):679-82.

Collins AL, Greenfield VY, Bye JK, Linker KE, Wang AS, Wassum KM. Dynamic mesolimbic dopamine signaling during action sequence learning and expectation violation. Sci Rep. 2016 Feb 12;6:20231.

Costall B, Naylor RJ, Pycock C. Non-specific supersensitivity of striatal dopamine receptors after 6-hydroxydopamine lesion of the nigrostriatal pathway. Eur J Pharmacol. 1976;35(2):276-283.

da Silva JA, Tecuapetla F, Paixão V, Costa RM. Dopamine neuron activity before action initiation gates and invigorates future movements. Nature. 2018;554(7691):244-248.

DeLong MR, Crutcher MD, Georgopoulos AP. Relations between movement and single cell discharge in the substantia nigra of the behaving monkey. J Neurosci. 1983 Aug;3(8):1599-606.

Djaldetti R, Ziv I, Melamed E. The mystery of motor asymmetry in Parkinson's disease. Lancet Neurol. 2006;5(9):796-802.

780 Diuk C, Tsai K, Wallis J, Botvinick M, Niv Y. Hierarchical learning induces two simultaneous,
781 but separable, prediction errors in human basal ganglia. J Neurosci. 2013;33(13):5797-5805.
782 Dodson PD, Dreyer JK, Jennings KA, Syed EC, Wade-Martins R, Cragg SJ, Bolam JP, Magill
783 PJ. Representation of spontaneous movement by dopaminergic neurons is cell-type selective and
784 disrupted in parkinsonism. Proc Natl Acad Sci U S A. 2016 Apr 12;113(15):E2180-8.
785 Dowd E, Dunnett SB. Comparison of 6-hydroxydopamine-induced medial forebrain bundle and
786 nigrostriatal terminal lesions in a lateralised nose-poking task in rats. Behav Brain Res. 2005 Apr
787 15;159(1):153-61.
788 Ehringer H, Hornykiewicz O. [Distribution of noradrenaline and dopamine (3-hydroxytyramine)
789 in the human brain and their behavior in diseases of the extrapyramidal system]. Klin
790 Wochenschr. 1960 Dec 15;38:1236-9
791 Fox ME, Mikhailova MA, Bass CE, et al. Cross-hemispheric dopamine projections have
792 functional significance. Proc Natl Acad Sci U S A. 2016;113(25):6985-6990
793 Freed CR, Yamamoto BK. Regional brain dopamine metabolism: a marker for the speed,
794 direction, and posture of moving animals. Science. 1985;229(4708):62-65.
795 Grace AA, Bunney BS. The control of firing pattern in nigral dopamine neurons: single spike
796 firing. J Neurosci. 1984;4(11):2866-2876.
797 Ghosh KK, Burns LD, Cocker ED, Nimmerjahn A, Ziv Y, Gamal AE, Schnitzer MJ. Miniaturized
798 integration of a fluorescence microscope. Nat Methods. 2011 Sep 11;8(10):871-8.
799 Hallett M, Khoshbin S. A physiological mechanism of bradykinesia. Brain. 1980 Jun;103(2):301-
800 14.
801 Hernandez LF, Obeso I, Costa RM, Redgrave P, Obeso JA. Dopaminergic Vulnerability in
802 Parkinson Disease: The Cost of Humans' Habitual Performance. Trends Neurosci. 2019
803 Jun;42(6):375-383.
804 Howe MW, Dombeck DA. Rapid signalling in distinct dopaminergic axons during locomotion
805 and reward. Nature. 2016;535(7613):505-510. doi:10.1038/nature18942

Howe MW, Tierney PL, Sandberg SG, Phillips PE, Graybiel AM. Prolonged dopamine signalling in striatum signals proximity and value of distant rewards. Nature. 2013;500(7464):575-579

Jankovic J. Parkinson's disease: clinical features and diagnosis. J Neurol Neurosurg Psychiatry. 2008 Apr;79(4):368-76.

Jaeger CB, Joh TH, Reis DJ. The effect of forebrain lesions in the neonatal rat: survival of midbrain dopaminergic neurons and the crossed nigrostriatal projection. J Comp Neurol. 1983;218(1):74-90.

Jin X, Costa RM. Start/stop signals emerge in nigrostriatal circuits during sequence learning. Nature. 2010;466(7305):457-462.

Kang SY, Wasaka T, Shamim EA, Auh S, Ueki Y, Lopez GJ, Kida T, Jin SH, Dang N, Hallett M. Characteristics of the sequence effect in Parkinson's disease. Mov Disord. 2010 Oct 15;25(13):2148-55.

Kitama T, Ohno T, Tanaka M, Tsubokawa H, Yoshida K. Stimulation of the caudate nucleus induces contraversive saccadic eye movements as well as head turning in the cat. Neurosci Res. 1991 Oct;12(1):287-92.

Klaus A, Martins GJ, Paixao VB, Zhou P, Paninski L, Costa RM. The Spatiotemporal Organization of the Striatum Encodes Action Space. Neuron. 2017 Aug 30;95(5):1171-1180.e7.

Lahiri AK, Bevan MD. Dopaminergic Transmission Rapidly and Persistently Enhances Excitability of D1 Receptor-Expressing Striatal Projection Neurons. Neuron. 2020 Apr 22;106(2):277-290.e6.

Lau B, Monteiro T, Paton JJ. The many worlds hypothesis of dopamine prediction error: implications of a parallel circuit architecture in the basal ganglia. Curr Opin Neurobiol. 2017;46:241-247.

Lee RS, Mattar MG, Parker NF, Witten IB, Daw ND. Reward prediction error does not explain movement selectivity in DMS-projecting dopamine neurons. Elife. 2019;8:e42992.

831 Mazzoni, P., Hristova, A. & Krakauer, J. W. Why don't we move faster? Parkinson's disease,
832 movement vigor, and implicit motivation. J. Neurosci. 27, 7105–7116 (2007).
833 Monje MHG, Sánchez-Ferro Á, Pineda-Pardo JA, Vela-Desojo L, Alonso-Frech F, Obeso JA.
834 Motor Onset Topography and Progression in Parkinson's Disease: the Upper Limb Is First. Mov
835 Disord. 2021 Jan 20.
836 Morrish PK, Sawle GV, Brooks DJ. Regional changes in [18F]dopa metabolism in the striatum
837 in Parkinson's disease. Brain. 1996 Dec;119 (Pt 6):2097-103.
838 Moss M, Zatka-Has P, Harris KD, Carandi M, Lak A. Dopamine axons to dorsal striatum
839 enconde contralateral stimuli and actions, 2020 (bioRxiv)
840 Niv Y, Daw ND, Joel D, Dayan P. Tonic dopamine: opportunity costs and the control of response
841 vigor. Psychopharmacology (Berl). 2007;191(3):507-520.
842 Panigrahi B, Martin KA, Li Y, Graves AR, Vollmer A, Olson L, Mensh BD, Karpova AY, Dudman
843 JT. Dopamine Is Required for the Neural Representation and Control of Movement Vigor. Cell.
844 2015 Sep 10;162(6):1418-30.
845 Parker NF, Cameron CM, Taliaferro JP, Lee J, Choi JY, Davidson TJ, Daw ND, Witten IB.
846 Reward and choice encoding in terminals of midbrain dopamine neurons depends on striatal
847 target. Nat Neurosci. 2016 Jun;19(6):845-54.
848 Palmiter RD. Dopamine signaling in the dorsal striatum is essential for motivated behaviors:
849 lessons from dopamine-deficient mice. Ann N Y Acad Sci. 2008;1129:35-46.
850 Poulin JF, Caronia G, Hofer C, et al. Mapping projections of molecularly defined dopamine
851 neuron subtypes using intersectional genetic approaches. Nat Neurosci. 2018;21(9):1260-1271.
852 Romo R, Schultz W. Dopamine neurons of the monkey midbrain: contingencies of responses
853 to active touch during self-initiated arm movements. J Neurophysiol. 1990;63(3):592-606.
854 Roggendorf J, Chen S, Baudrexel S, van de Loo S, Seifried C, Hilker R. Arm swing asymmetry
855 in Parkinson's disease measured with ultrasound based motion analysis during treadmill gait. Gait
856 Posture. 2012 Jan;35(1):116-20.

857 Saunders BT, Richard JM, Margolis EB, Janak PH. Dopamine neurons create Pavlovian
858 conditioned stimuli with circuit-defined motivational properties. Nat Neurosci. 2018
859 Aug;21(8):1072-1083.
860 Schultz W. Getting formal with dopamine and reward. Neuron. 2002;36(2):241-263.
861 Schultz, W., Ruffieux, A. & Aebischer, P. The activity of pars compacta neurons of the monkey
862 substantia nigra in relation to motor activation. Exp Brain Res 51, 377–387 (1983).
863 Schwarcz R, Fuxe K, Agnati LF, Hökfelt T, Coyle JT. Rotational behaviour in rats with unilateral
864 striatal kainic acid lesions: a behavioural model for studies on intact dopamine receptors. Brain
865 Res. 1979 Jul 20;170(3):485-95.
866 Stott SR, Barker RA. Time course of dopamine neuron loss and glial response in the 6-OHDA
867 striatal mouse model of Parkinson's disease. Eur J Neurosci. 2014 Mar;39(6):1042-56.
868 Shah VV, McNames J, Mancini M, Carlson-Kuhta P, Spain RI, Nutt JG, El-Gohary M, Curtze C,
869 Horak FB. Quantity and quality of gait and turning in people with multiple sclerosis, Parkinson's
870 disease and matched controls during daily living. J Neurol. 2020 Apr;267(4):1188-1196.
871 Tecuapetla F, Matias S, Dugue GP, Mainen ZF, Costa RM. Balanced activity in basal ganglia
872 projection pathways is critical for contraversive movements. Nat Commun. 2014 Jul 8;5:4315.
873 Takahashi YK, Langdon AJ, Niv Y, Schoenbaum G. Temporal Specificity of Reward Prediction
874 Errors Signaled by Putative Dopamine Neurons in Rat VTA Depends on Ventral Striatum. Neuron.
875 2016;91(1):182-193.
876 Weintraub D, Simuni T, Caspell-Garcia C, et al. Cognitive performance and neuropsychiatric
877 symptoms in early, untreated Parkinson's disease. Mov Disord. 2015;30(7):919-927.
878 Zhou P, Resendez SL, Rodriguez-Romaguera J, Jimenez JC, Neufeld SQ, Giovannucci A,
879 Friedrich J, Pnevmatikakis EA, Stuber GD, Hen R, Kheirbek MA, Sabatini BL, Kass RE, Paninski
880 L. Efficient and accurate extraction of in vivo calcium signals from microendoscopic video data.
881 Elife. 2018 Feb 22;7:e28728.

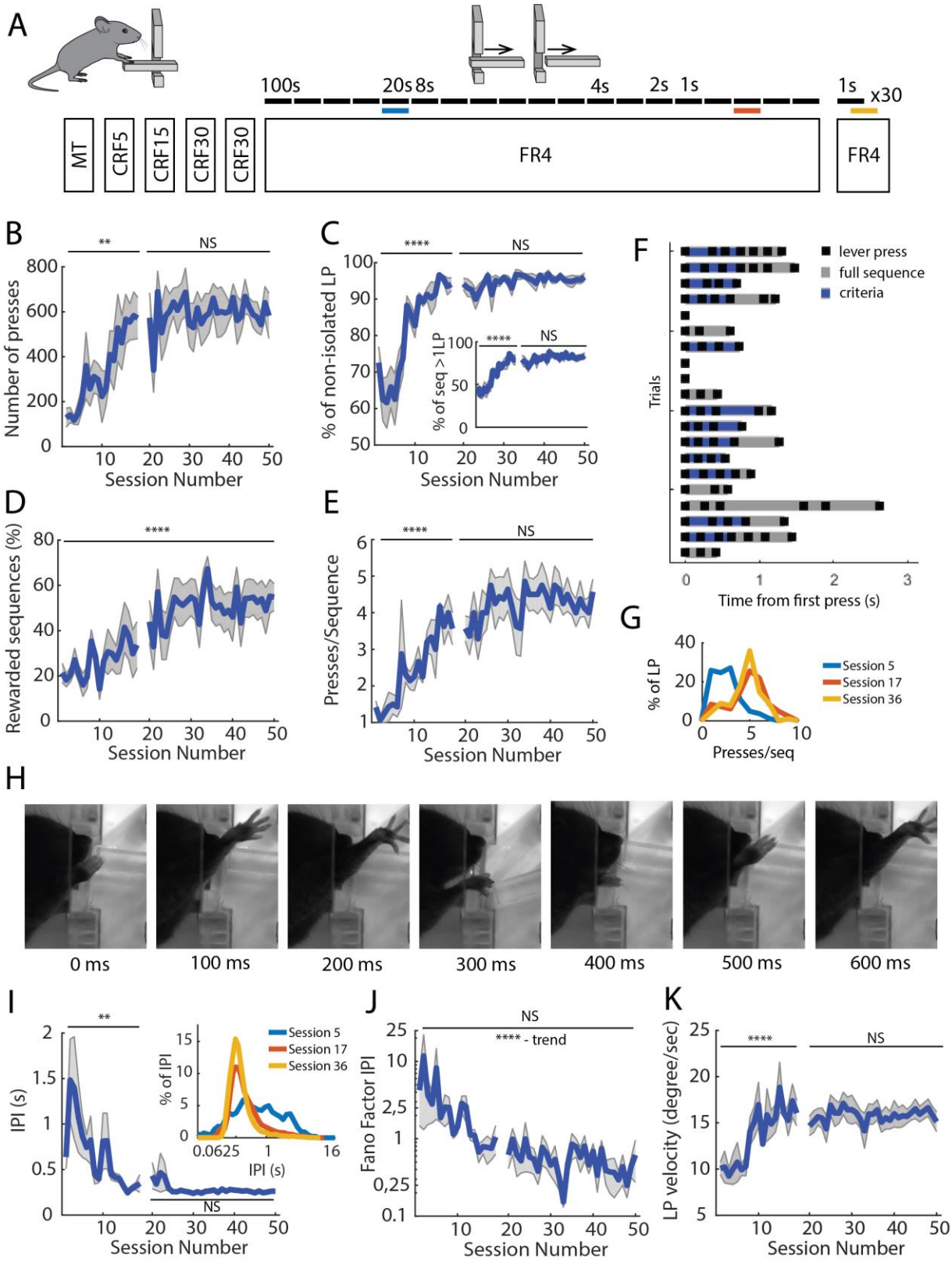

Figure 1

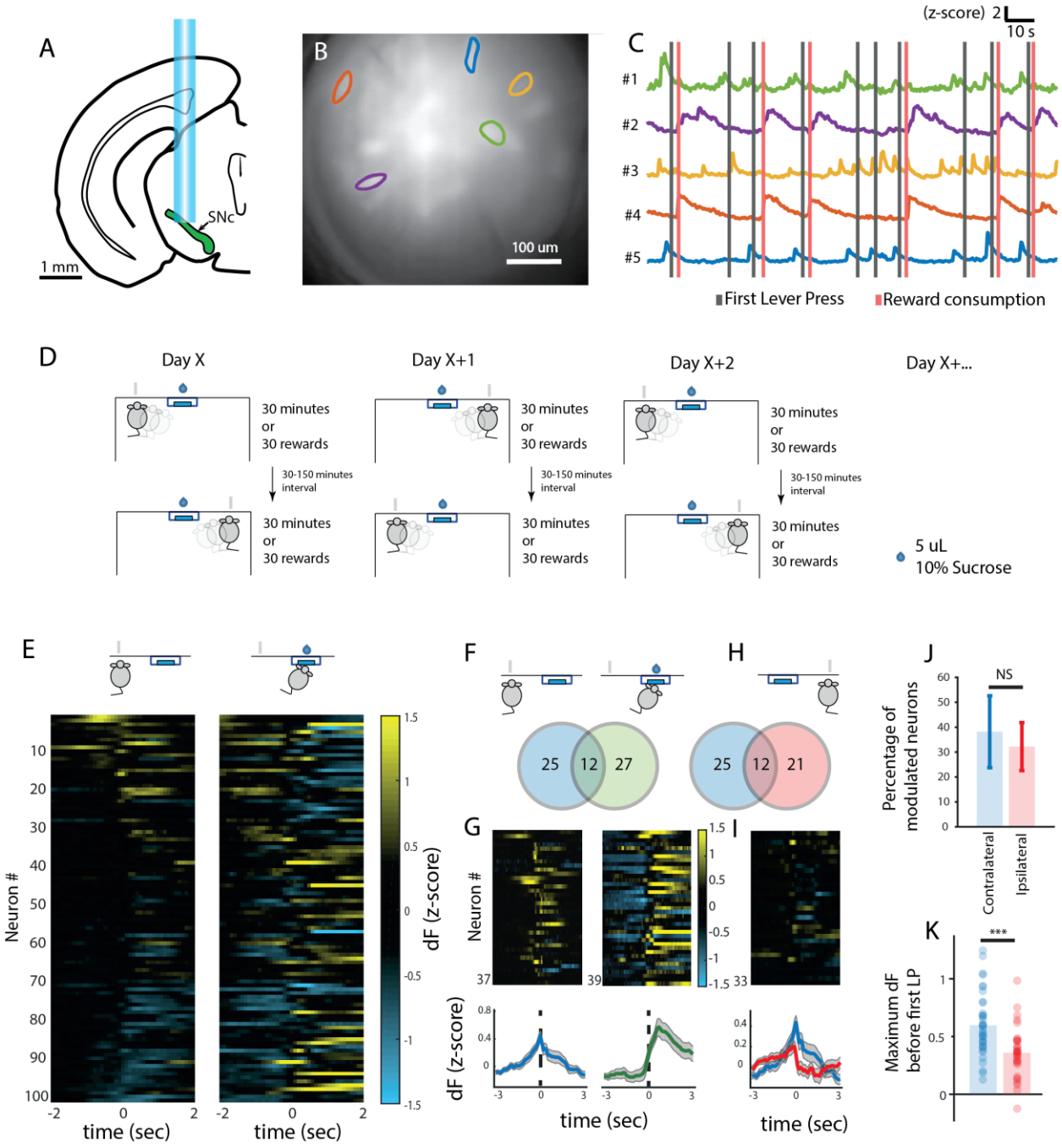

Figure 2

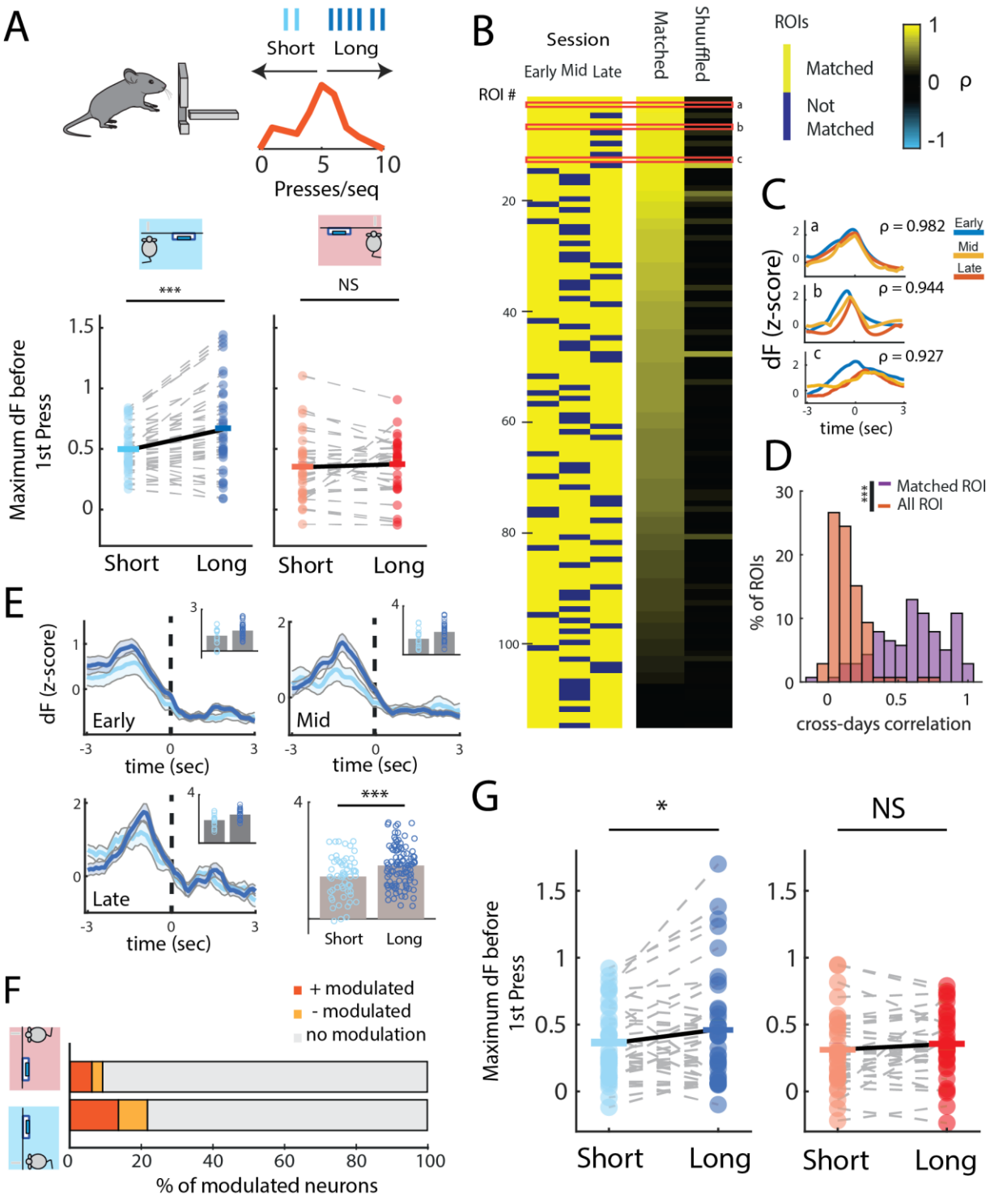

Figure 3

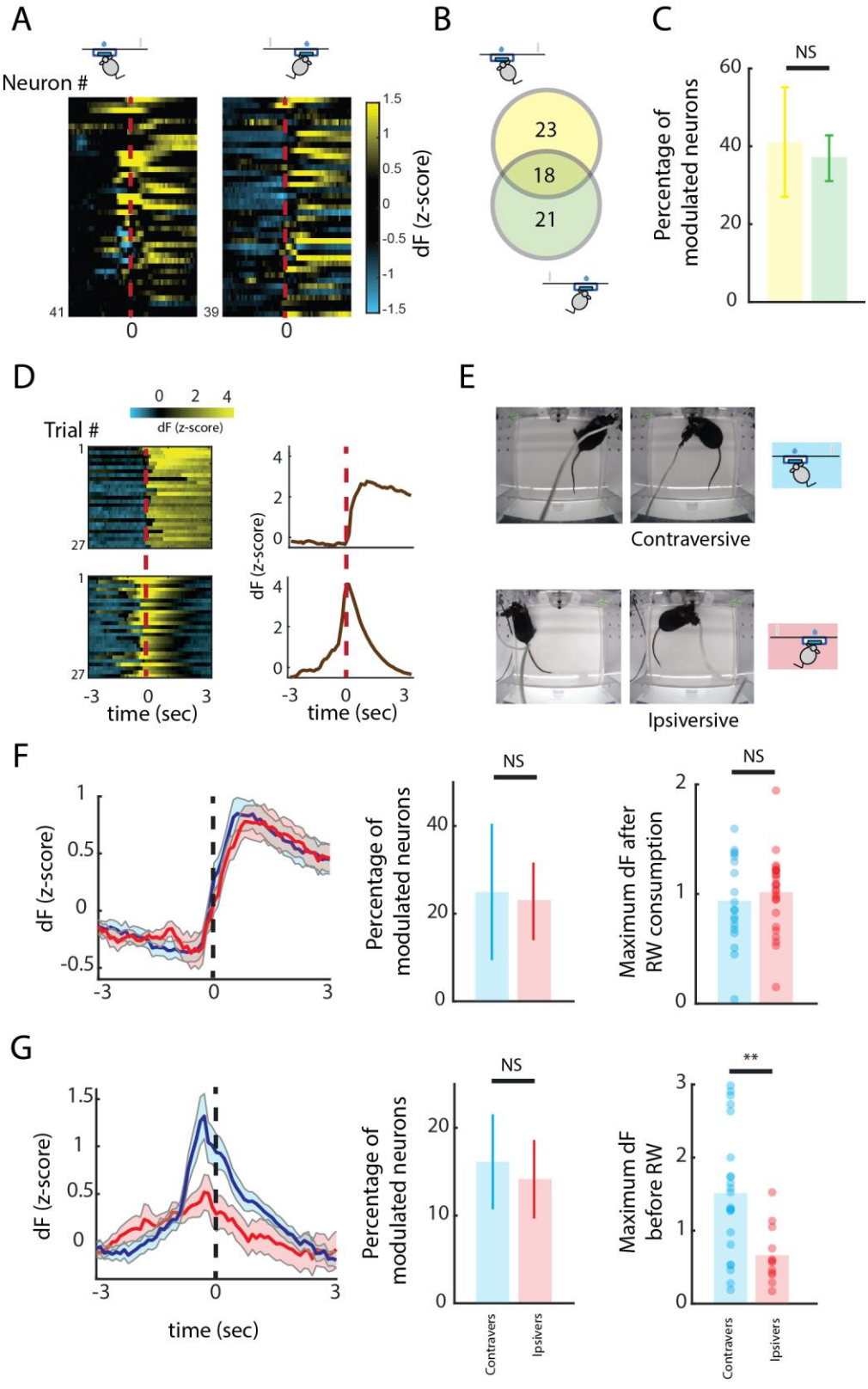

Figure 4

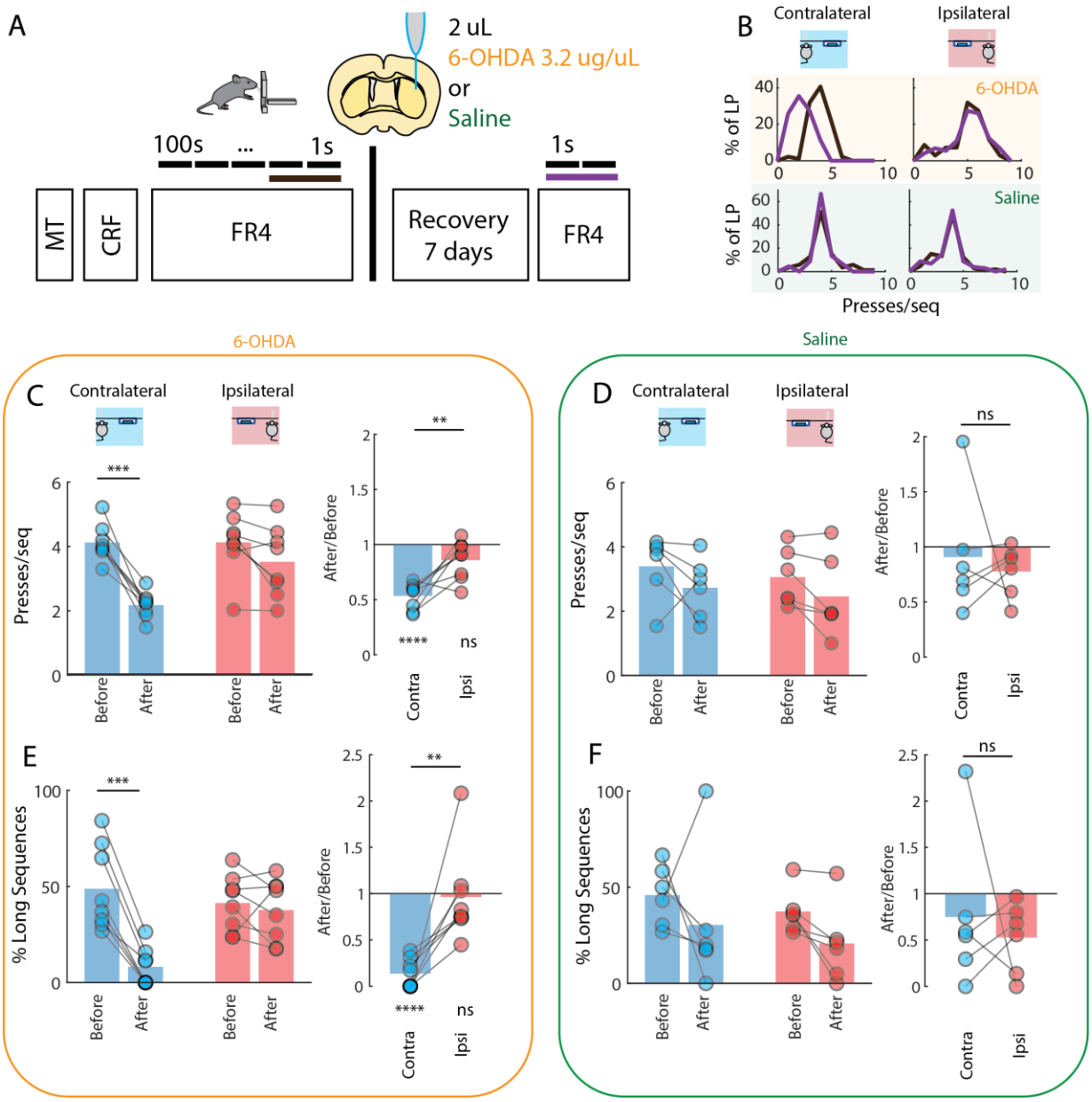

Figure 5